Available online at www.sciencedirect.com
SCIENCE DIRECT®
Physica D 185 (2003) 158–174
PHYSICA D
www.elsevier.com/locate/physd

A dissipative one-dimensional collision model with intermediate energy storage

J. Dunkel [a,*], W. Ebeling [a], J.W.P. Schmelzer [b,c], G. Röpke [b,c]

[a] *Institute of Physics, Humboldt-University, Newtonstraße 15, D-12489 Berlin, Germany*
[b] *Department of Physics, University of Rostock, 18051 Rostock, Germany*
[c] *Bogoliubov Laboratory of Theoretical Physics, Joint Institute for Nuclear Research, 141980 Dubna, Russia*

Received 27 September 2002; accepted 2 May 2003
Communicated by R.P. Behringer

Abstract

We study a simple model for a dissipative collision process of two one-dimensional chains, consisting of point-particles. In this model, the particles interact with their nearest neighbors via nonlinear Morse potentials. In addition, each particle is subject to nonlinear friction, modeling the transfer of energy between the translational degree of freedom and energy depots, representing further (internal) degrees of freedom. Depending on the momentary state of the system, this energy exchange mechanism can decrease or increase the kinetic energy of the particles on the cost of the depots. In particular, the clusters are assumed to have the ability to store parts of their initial energy in the depots. In later stages of a collision process, the stored depot energy can be used for an acceleration of the fragments, i.e., it can be converted into kinetic energy of motion. Both, analytically and by means of computer simulations, we investigate the dependence of the fragmentation channels, observed after the collisions, on different initial conditions (e.g. initial particle energy, cluster size) and system parameters.

PACS: 05.45.−a; 24.10.−i; 25.70.−z

Keywords: Energy storage in depots; Dissipative cluster collisions; Fragmentation channels

1. Introduction

Collision and scattering experiments are among the most powerful tools allowing to investigate the physical properties, the structure and the laws governing the behavior of matter on different macroscopic and microscopic length scales [1–4]. Traditionally, the theory of particle collision processes is well-investigated on classical and non-relativistic as well as on relativistic and quantum levels for the case that the interactions, which determine the outcome of the collision process, are realized by conservative forces (elastic collisions [5]).

With regard to non-conservative or dissipative collision processes (e.g. [6]), the whole situation is quite different. In contrast to the scattering theory dealing with conservative forces, the theory of dissipative collisions is far

* Corresponding author.
E-mail address: dunkel@physik.hu-berlin.de (J. Dunkel).

0167-2789/$ – see front matter © 2003 Elsevier B.V. All rights reserved.
doi:10.1016/S0167-2789(03)00233-1

from being complete. One reason for that is, for example, the absence of conserved quantities like energy, when also taking into account dissipation. In such cases exact analytical predictions become extremely difficult or even impossible. Considering these difficulties, one could certainly ask the question: why are we interested in dissipative (collision) processes at all? The simple answer is, that actually all macroscopic processes are of dissipative nature, i.e., they include complex energy exchange mechanisms such as friction or thermal pumping. Sometimes of course, the influence of dissipation can be neglected, since it reveals its presence at time scales which are beyond the observational time span. On the other hand, if we think of physical, chemical and biological non-equilibrium systems, where dissipation is the driving force of pattern formation on macroscopic as well as on microscopic length scales [7], then one may expect that dissipation of energy also causes peculiarities in collision processes of matter, which are absent in purely conservative systems.

In preceding investigations [8,9], based on the analysis of two colliding linear chains of particles, it was found, indeed, that dissipation may lead to a large variety of fragmentation channels, not observable in purely conservative processes of similar kind. In the cited papers, the dissipation was modeled by a law similar to that valid for the motion of a body in viscous media. Now, the questions arises, whether the diversity in the number of fragmentation channels, as observed in [8,9], is only due to special dissipative force employed there, or whether this is a rather general effect also observable for other types of friction. In this sense, we extend the analysis by considering not only conventional friction (resulting in a decrease of the mechanical energy of motion), but also so-called negative friction, leading to an increase of the kinetic energy. To this end, we shall use a simple nonlinear friction model, which was introduced in [10], as generalization of Rayleigh's model of negative friction [11].

In the present work, we investigate a one-dimensional, non-relativistic model of dissipative collision processes. Our model simulates the following physical situation. We start with two clusters moving towards each other. The first cluster consists of N_1 particles, each possessing the same initial velocity value $+v_0$, while the second cluster contains N_2 particles, each starting with velocity $-v_0$. After the collision of two such chains, we expect to find one, two, or, in general, several clusters.

The scattering process itself is dissipative in the following sense. In our model we assume, that during collisions the kinetic energy of the particles cannot only be transformed into conservative potential energy, but that, additionally, also internal degrees of freedom, modeled by energy depots, may be excited. Moreover, we assume that the energy stored in such depots can be used for accelerating the particles during the scattering, until they reach the initial value of the kinetic energy again (in a sense, one could say the depots work like the battery of car). The conversion of kinetic energy of motion into depot energy, and vice versa, will be realized by including a nonlinear velocity-dependent friction force, $f_{\mathrm{dis}}(v)$, in the Newtonian equations of motions. Hence, our model is dissipative with respect to the structure of the dynamical equations, but, nevertheless, it can also be considered as energy-conserving in total. The latter fact we are going to clarify below by including a depot energy term in the balance equation of energy.

As already mentioned, this article extends previous work on dissipative collisions [8,9] and active Morse chains [12,13]. The primary aim is to learn about the interplay between dissipative and conservative forces and, of course, about the resulting effects. Although our relatively simple model is still far away from real systems, we consider it appropriate in order to gain a deeper insight into the essential mechanisms. In the investigations, we primarily use the methods of qualitative analysis as known from nonlinear dynamics and, to a great extent, numerical simulations.

The paper is organized as follows. In Section 2 we introduce the model. Section 3 is exclusively dedicated to the analysis of two-particle-collisions. For this case, analytical results can be derived, which turn out to be useful for the understanding of fragmentation involving higher numbers of particles, too. In Section 4 we present numerical results for collisions of longer chains. Finally, Section 5 contains a brief summary and an outlook on possible future research in the present field.

2. The model

2.1. Basic equations and assumptions

We consider a set of N point-like particles with identical masses m moving in the one-dimensional laboratory frame Σ. At time t each particle is described by a coordinate $x_i(t) \in \mathbb{R}$ (where $i = 1, \ldots, N$) and its velocity $v_i(t) \in \mathbb{R}$ in Σ. In our model we assume that the dynamics of the particles in Σ is governed by the Newtonian equations of motion

$$\dot{x}_i = v_i, \tag{1a}$$

$$\dot{v}_i = \frac{1}{m} F_i - \gamma(v_i) v_i, \tag{1b}$$

where $\dot{v}_i = \mathrm{d}v_i/\mathrm{d}t$. Each particle can interact with its nearest neighbors via conservative forces F_i and is additionally subject to nonlinear friction represented by the last term in (1b). The conservative interaction force F_i can be derived from the potential energy function U of the system by

$$-F_i = \frac{\partial}{\partial x_i} U = \frac{\partial}{\partial x_i} \sum_{j=1}^{N-1} U_j(x_{j+1} - x_j). \tag{2}$$

For the pair potentials $U_i(r_i) = U_i(x_{i+1} - x_i)$ we assume

$$U_i(r_i) = \frac{a}{2b}[\mathrm{e}^{-b(r_i-\sigma)} - 1]^2, \tag{3}$$

representing so-called Morse potentials, where a, b and σ are positive parameters.

Originally, the Morse potential (3) was introduced to describe diatomic molecules [14]. Inserted into Schrödinger's equation it allows an exact calculation of their energy spectrum. We note, that the Morse potential can also be considered as generalization of Toda's exponential potential [15], which has been extensively studied before [16]. As evident from (3), and also illustrated in Fig. 1 the Morse potential possesses at $r_i = \sigma$ the only minimum $U_i(\sigma) = 0$ and tends asymptotically to

$$\varepsilon = \frac{a}{2b} \tag{4}$$

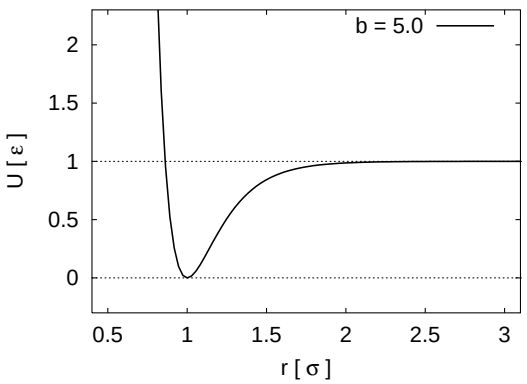

Fig. 1. Morse potential as used in the numerical simulations. The parameter b is given in units σ^{-1}.

at $r_i \to \infty$. The angular frequency ω near the minimum is defined by

$$\omega^2 = \frac{1}{m}\frac{\mathrm{d}^2 U_i(\sigma)}{\mathrm{d}r_i^2} = \frac{ab}{m}. \tag{5}$$

For subsequent discussion it is convenient to use a characteristic system of units (c.u.), such that $m = 1$, $\sigma = 1$ and $\varepsilon = 1$. Hence, the characteristic unit time τ of our model reads

$$\tau = \sigma\sqrt{\frac{m}{\varepsilon}} = 1 \quad (\text{in c.u.}), \tag{6}$$

and we find $\omega^2 = 2b^2$ (in c.u.). In order to justify our restriction on nearest neighbor (n.n.) interactions, we have to choose a sufficiently large parameter value b. As we can see in Fig. 1, parameter values $b \geq 5\sigma^{-1}$ are satisfactory, since then the Morse interaction force decays sufficiently fast.

2.2. The depot model

Having discussed the conservative interaction in our model so far, we now turn the attention to the dissipative forces also appearing in the equations of motion (1). In this work we intend to use the following nonlinearly velocity-dependent friction coefficient

$$\gamma(v) = \gamma_0\left(1 - \frac{\kappa + \mu}{\kappa + v^2}\right) = \gamma_0\frac{v^2 - \mu}{\kappa + v^2}, \tag{7}$$

where κ and γ_0 are positive parameters, while μ can also take negative values. This friction coefficient (see also Fig. 2) was originally proposed to describe active Brownian particles carrying internal energy depots [10]. The parameter γ_0 is the usual viscous friction coefficient and has the meaning of an inverse relaxation time. As evident from the r.h.s. of (7), the parameter μ plays the role of a bifurcation parameter. It is an important aspect, that we identify $\mu = v_0^2$ in our model, where v_0 is the absolute value of the initial velocity; i.e., there is no dissipation in the initial state. Hence, the friction coefficient $\gamma(v)$ is negative, if the absolute velocity of a particle is smaller than v_0, and positive if $|v| > v_0$. From the physical point view this means, that during the first stage of the collision, when the particles are accelerated to $|v| > v_0$ due to the attractive part of the Morse potential, some energy flows into non-translational degrees of freedom (the depots) via a dissipative mechanism represented by (7). On the other

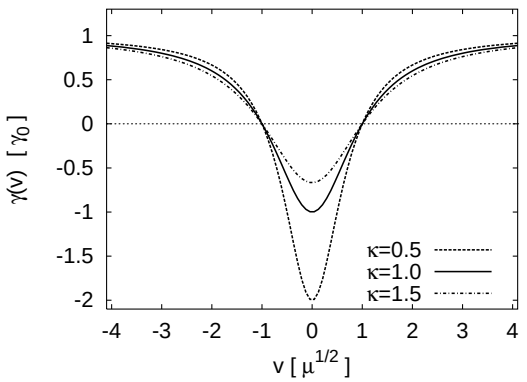

Fig. 2. Shape of the friction coefficient $\gamma(v)$ for different values of κ in units $[\kappa] = \mu$. The region, where $\gamma(v) < 0$ holds, corresponds to the transformation of stored depot energy into translational kinetic energy of motion. On the other hand, if $\gamma(v)$ is positive, then kinetic energy is transformed into (dissipative) depot energy.

hand, in the second stage, when the particles are slowed down by the repulsive part of the Morse potential, they can regain kinetic energy from depot energy stored before. Finally, we note, that the remaining parameter κ is related to the ratio between internal dissipation and conversion of depot energy into kinetic energy of motion. For further details regarding this parameter, we refer the reader to [10,17].

In principle, for the time being, it is sufficient to consider (7) as a simple nonlinear friction model depending on a particle's kinetic energy and converging to the viscous friction coefficient γ_0, if $v^2 \to \infty$. Since a variation of κ does not cause qualitative changes of the friction coefficient, we are going to fix $\kappa = 1\varepsilon m^{-1}$ (corresponding to $\kappa = 1$ in c.u.) during all computer simulations.

Another convenient form of the dynamical equations follows by introducing a dissipative potential

$$U_{\mathrm{dis}}(v) := \frac{m}{2}\gamma_0 \left[v^2 - \mu - (\kappa + \mu) \ln\left(\frac{\kappa + v^2}{\kappa + \mu}\right)\right], \tag{8}$$

from which we can derive the dissipative force by

$$f_{\mathrm{dis}} = -\frac{\partial}{\partial v} U_{\mathrm{dis}}. \tag{9}$$

In case of $\mu > 0$, the bistable potential $U_{\mathrm{dis}}(v)$ has two minima at $\pm v_0 = \pm\sqrt{\mu}$, corresponding to the initial conditions used in our theoretical scattering experiments. The shape of $U_{\mathrm{dis}}(v)$ can be seen in Fig. 3. For non-interacting particles, i.e., if $|x_{i+1} - x_i| \to \infty$ or $|x_{i+1} - x_i| = 1$ (in c.u.), as for instance observable after a quasi-elastic collision, we have

$$\dot{v}_i = f_{\mathrm{dis}}(v_i) = \gamma_0 \frac{\mu - v_i^2}{\kappa + v_i^2} v_i. \tag{10}$$

In other words, for negligible conservative interaction forces, this type of friction (or pumping, respectively) leads again to the two stable velocities $\pm v_0 = \pm\sqrt{\mu}$, corresponding to the initial velocities or minima of the dissipative potential, respectively.

Finally, let us consider the energy balance. By multiplication of Eq. (1b) with the velocity v_i and subsequent summation, we obtain

$$\frac{\mathrm{d}}{\mathrm{d}t}\left(\frac{m}{2}\sum_i v_i^2 + U\right) = -\sum_i \gamma(v_i)\, v_i^2. \tag{11}$$

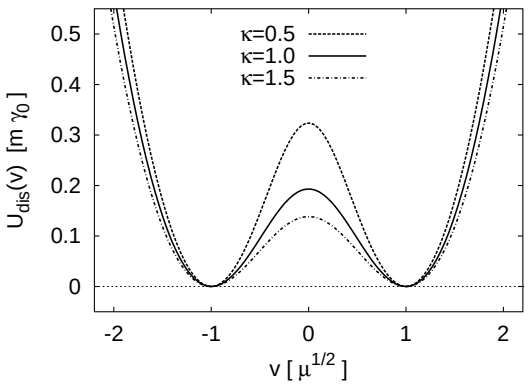

Fig. 3. Shape of the dissipative potential as defined in Eq. (8).

Introducing by definition the energy in the depots

$$E_{\mathrm{dis}}(t) := \int_0^t \mathrm{d}s \sum_i \gamma(v_i(s))v_i(s)^2, \tag{12}$$

we can rewrite (11) as

$$\frac{\mathrm{d}}{\mathrm{d}t}\left[\frac{m}{2}\sum_i v_i^2 + U + E_{\mathrm{dis}}(t)\right] = 0. \tag{13}$$

This relation expresses the balance equation for the total energy (including the dissipative energy E_{dis} stored in the depots). We note, that for initial states with $v_i(0) = \pm\sqrt{\mu}$ always $E_{\mathrm{dis}}(0) = 0$ holds.

Thus, we may summarize the physics contained in the model as follows. We have introduced a depot which may store dissipative energy. In the first part of the collision process our systems stores energy in the depots, which can be regained later. In a sense, the dissipative depots work like a battery, that, on the one hand, can be charged using a dynamo and, on the other hand, also provides energy for the acceleration of the particles.

2.3. Initial conditions and fragmentation channels

In real collision or scattering experiments the initial states of the collision partners essentially determine the results finally observed. In this work we investigate the collision of two one-dimensional dissipative Morse chains governed by the dynamical equations (1), while concentrating on the following initial situation in the laboratory frame Σ.

At time $t = 0$ the first chain contains N_1 particles moving with initial velocities $v_i(0) = +\sqrt{\mu}$ $(i = 1, \ldots, N_1)$ to the right and the second one consists of N_2 particles moving with $v_j(0) = -\sqrt{\mu}$ $(j = N_1 + 1, \ldots, N)$ to the left. We shall also use the notation $[N_1, N_2]$ to symbolize this configuration. Consequently, the initial kinetic energy E_{in} of each particle simply reads

$$E_{\mathrm{in}} = \tfrac{1}{2}\mu. \tag{14}$$

Changing the parameter μ means a change of the initial energy in our computer experiments. Since μ is the main bifurcation parameter in the theory presented, the initial kinetic energy is the decisive quantity for the determination of the outcome of the scattering process.

The particle number $N = N_1 + N_2$ is conserved during the whole process. The distance $d(t)$ between the chains is defined as

$$d(t) = x_{N_1+1}(t) - x_{N_1}(t). \tag{15}$$

In our computer experiments we shall always start with two chains (or clusters), separated by a large initial distance, more exactly $d(0) \gg \sigma$ (see also Fig. 4). Furthermore, the initial distance between n.n. within the same cluster is assumed to be 1σ, corresponding to the equilibrium length of the Morse potentials. The time t_{col} of the first collision of the chains is approximately given by

$$t_{\mathrm{col}} \approx \frac{d(0)}{2|v(0)|} = \frac{d(0)}{2\sqrt{\mu}}. \tag{16}$$

It is an useful quantity in order to estimate the duration of the computer experiments. According to the special initial conditions the two chains are quasi-equilibrated at time $t = 0$. While they are moving towards each other, their internal structure does not essentially change as long as $t \ll t_{\mathrm{col}}$; but, as soon as their distance becomes sufficiently small, $t \lesssim t_{\mathrm{col}}$, the local equilibrium states of the chains are destroyed, and the whole system has to reorganize

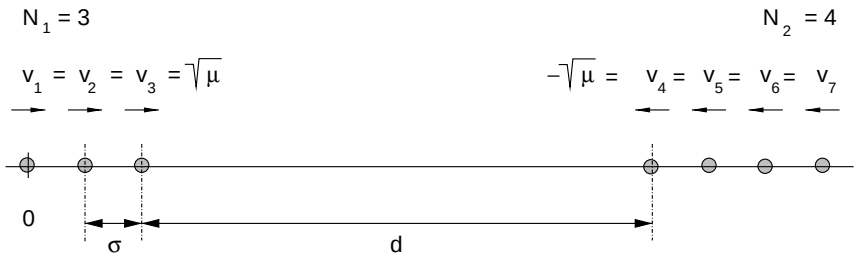

Fig. 4. Schematic representation of the initial configuration at time $t = 0$ for $N = 7$ particles.

after the collision. Our aim is to illuminate the interplay of dissipation and conservative interaction during the recombination process.

In agreement with the standard terminology of collision theory we shall refer to each outcome of a collision experiment as fragmentation channel. Let us, for example, imagine an initial configuration $[N_1, N_2]$ with $N = N_1 + N_2$ particles. Then each final state (fragmentation channel)

$$\phi = [n_1, \ldots, n_j] \tag{17}$$

consisting of j clusters with different sizes n_k must contain N particles, too. Thus, we have

$$N = \sum_{k=1}^{j} n_k. \tag{18}$$

For example, in case of $N = 3$ particles possible fragmentation channels of the collision experiment are

$$\phi \in \{[3], [2, 1], [1, 2], [1, 1, 1]\}. \tag{19}$$

We conclude this section with some remarks on the numerical simulations. For all numerical simulations of the dynamical system (1) we used the classical Runge–Kutta algorithm with discrete time intervals of length $\mathrm{d}t = 0.0001\tau$. The parameter b of the Morse potential and the parameter κ of the friction coefficient were always set to values $b = 5.0$ and $\kappa = 1.0$ (in c.u.). This choice of parameters corresponds to the Morse potential as drawn in Fig. 1 and to the solid line in Fig. 2. Further, we defined that two n.n. particles are bound in the same cluster as long as their distance is smaller than 2σ. This definition is in agreement with the chosen parameter value $b = 5.0$, as we can learn from Fig. 1. Finally, we give below the compact mathematical form of the initial conditions as used in all numerical simulations (in c.u.):

(1) $x_1(0) = 0$, $x_i(0) = 1 + x_{i-1}(0)$ $(1 < i \leq N_1)$,
(2) $x_{N_1+1}(0) = x_{N_1}(0) + 20$, $x_i(0) = 1 + x_{i-1}(0)$ $(N_1 + 1 < i \leq N)$,
(3) $v_i(0) = +\sqrt{\mu}$ $(1 \leq i \leq N_1)$,
(4) $v_i(0) = -\sqrt{\mu}$ $(N_1 + 1 \leq i \leq N)$,

i.e., we always set $d(0) = 20$ (in c.u.).

3. The case $N = 2$

3.1. Fragmentation channels

In this section we deal with the simplest non-trivial case of two colliding particles corresponding to the initial state $\phi_{\mathrm{in}} = [1, 1]$. This situation does not seem very exciting at a first glance, but it has, however, the advantage that

it admits some analytical treatment. Moreover, we shall see later, that this case already exhibits some of the main features also met for $N > 2$.

For convenience, we use in this part instead of the laboratory system relative and center-of-mass (c.o.m.) coordinates defined by

$$r = x_2 - x_1, \qquad s = \tfrac{1}{2}(x_2 + x_1), \qquad v_r = v_2 - v_1, \qquad v_s = \tfrac{1}{2}(v_2 + v_1). \tag{20}$$

With respect to our characteristic unit system we obtain the full potential energy

$$U = U_1(r) = [\mathrm{e}^{-b(r-1)} - 1]^2. \tag{21}$$

Fixing initial conditions $v_1(0) = +\sqrt{\mu}$ and $v_2(0) = -\sqrt{\mu}$ in agreement with previous considerations yields $v_s(0) = 0$ and due to symmetry reasons also

$$v_s = 0, \qquad \dot{v}_s = 0 \quad \forall t > 0. \tag{22}$$

Thus, in this situation the only relevant dynamical equations are those for the change of the relative coordinate r given by

$$\dot{r} = v_r \tag{23a}$$

$$\dot{v}_r = 4[\mathrm{e}^{-b(r-1)} - 1]\,\mathrm{e}^{-b(r-1)} b + \gamma_0 \frac{4\mu - v_r^2}{4\kappa + v_r^2} v_r. \tag{23b}$$

Stationary solutions of the second equation (23b) are

$$S_0 = (r, v_r) = (1, 0), \qquad S_1 = (r, v_r) = (\infty, 2\sqrt{\mu}). \tag{24}$$

The first solution, S_0, is a stationary solution of the full dynamical system (23) and we can apply methods of the qualitative stability analysis. The eigenvalues $\lambda_{1/2}$ of the corresponding linearized system are given by

$$\lambda^{\pm} = \frac{1}{2\kappa}(\mu\gamma \pm \sqrt{\mu^2\gamma^2 - 16b^2\kappa^2}). \tag{25}$$

Because of $\mathrm{Re}\,\lambda^+ > 0$, solution S_0 represents an unstable fixed point $\forall \mu, \gamma > 0$. In the original particle picture, S_0 describes the situation, where the two particles are at rest while their distance is given by the equilibrium length 1σ. Due to its general instability, this type of stationary behavior will never be observed for initial conditions as applied in our studies.

From the mathematical point of view, the second solution, S_1, is not a stationary solution of the full dynamical system (23) because of the non-vanishing stationary velocity. Nevertheless, it is physically relevant in our model and corresponds to the situation, where the two particles overcome the binding energy after the collision and move into different directions (quasi-elastic collision). In contrast to S_0 the behavior described by S_1 is stable and can be observed for the initial conditions used in this work (see Fig. 5).

However, in course of our simulations we found out, that depending on the parameter values there may also exist another stable stationary solution representing a bound state of the two particles. More exactly, it corresponds to stationary anti-phase oscillations of the particles, while they form a cluster (see Fig. 6). For small stationary oscillations the oscillation amplitude can be analytically estimated using the following linearized version of (23):

$$\dot{r} = v_r, \tag{26a}$$

$$\dot{v}_r = -4b^2(r-1) + \frac{\gamma_0}{4\kappa}(4\mu - v_r^2) v_r. \tag{26b}$$

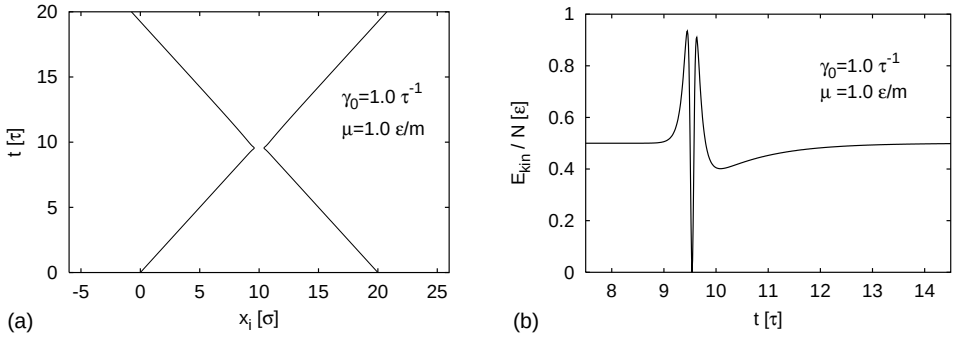

Fig. 5. (a) Traces of the two particles in case of a quasi-elastic collision. (b) Kinetic energy per particle during the collision as a function of time. Further parameter values are $b = 5$, $\kappa = 1$ (in c.u.).

In order to obtain (26), we additionally assumed, that $v_r^2 \ll 4\kappa$ holds, corresponding to weak pumping. In agreement with the linear approximation of the Morse interaction force in (26b), we are looking for a 2π-periodic approximation

$$v_r(t) = A \sin\theta(t) = A \sin(2bt) \tag{27}$$

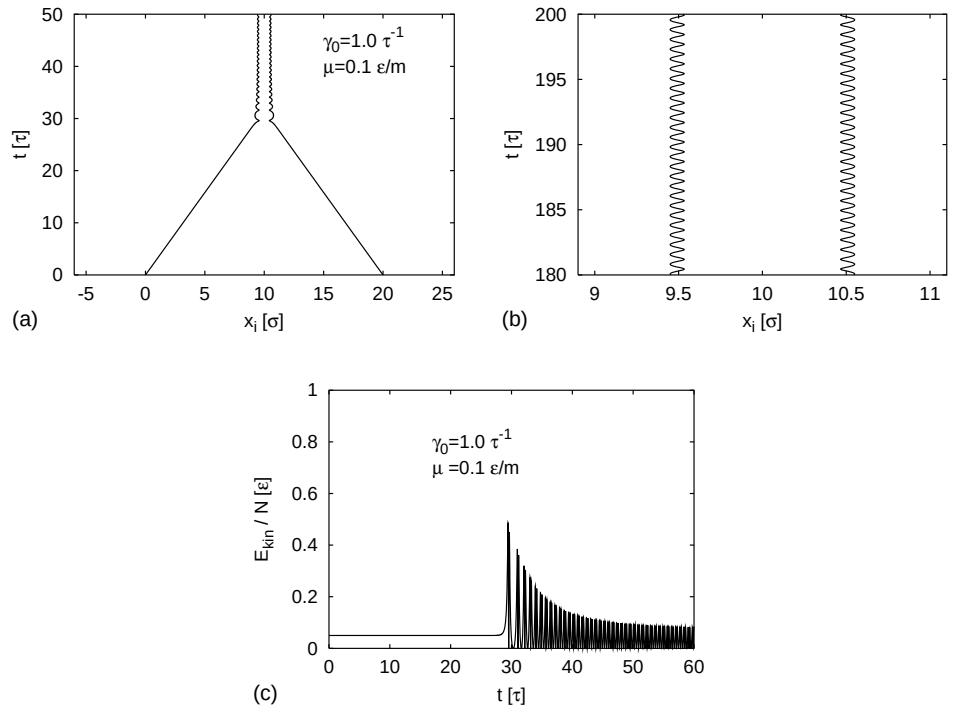

Fig. 6. (a) Traces of the two particles in case of a fusion. (b) The stationary (bound) state corresponds to (optical) anti-phase oscillations. According to the analytic estimate (31) the maximum/minimum distance between the particles is given by $r^{\pm} = (1 \pm 0.16)$ (in c.u.). (c) Kinetic energy per particle as a function of time. All three pictures are taken from the same simulation run (further parameter values are $b = 5$, $\kappa = 1$ in c.u.).

of the unknown exact stationary solution, such that

$$0 = \frac{\mathrm{d}}{\mathrm{d}t}\langle 2U(r) + T(v_r)\rangle = \frac{\mathrm{d}}{\mathrm{d}t}\left\langle 2U(r) + \frac{v_r^2}{2}\right\rangle = \left\langle \frac{\gamma_0}{4\kappa}(4\mu - v_r^2)v_r^2\right\rangle = \frac{1}{2\pi}\int_0^{2\pi} \mathrm{d}\theta \frac{\gamma_0}{4\kappa}(4\mu - v_r^2)v_r^2 \tag{28}$$

is fulfilled. The criterion (28) means nothing else but that for stationary solutions the temporal average of the mechanical energy must become constant [13]. Inserting (27) into (28) yields

$$0 = -\tfrac{3}{8}A^4 + 2A^2\mu, \tag{29}$$

which has the non-trivial solutions

$$A^{\pm} = \pm 4\sqrt{\tfrac{1}{3}\mu}. \tag{30}$$

Thus, we get as amplitudes of the relative oscillations

$$r^{\pm} = 1 + \frac{A^{\pm}}{2b} = 1 \pm \sqrt{\frac{4\mu}{3b^2}}. \tag{31}$$

For the parameter values used in Fig. 6 the analytical estimate is in acceptable agreement with the numerical result.

3.2. Basins of attraction

It remains to be discussed for which parameter values b, γ_0, μ, κ the two particles end up in the bound state or the separated state, respectively. The numerical results for fixed κ and b values are shown in Fig. 7. We shall now try to find an analytical estimate for the hyperplane separating the two corresponding parameter regions. To this end, we imagine the relative coordinate to represent a quasi-particle with unit mass (in c.u.) moving in the effective potential

$$V(r) = 2U(r). \tag{32}$$

We note, that this approach is the similar to that used before to calculate the stationary oscillation amplitude (31). But instead of the harmonic approximation of $V(r)$ employed in (26), we now choose a box-like approximation

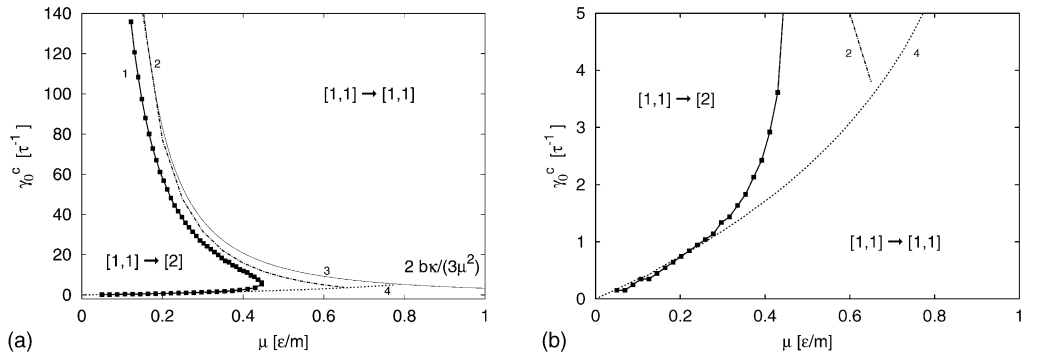

Fig. 7. Fragmentation channels for $N = 2$ particles and symmetric initial state $[N_1, N_2] = [1, 1]$. The solid curve 1 was numerically calculated. The dashed–dotted line 2 shows the analytical approximation of the upper branch and is obtained from the numerical solutions of the transcendental equation (47). The dotted curve 4 represents the analytical estimate for the lower branch according to (41). The other parameter values used here are $b = 5$, $\kappa = 1$ (in c.u.). (b) Enlarged section of the part (a).

$V_B(r)$ of the effective potential $V(r)$ reading

$$V_B(r) = \begin{cases} \infty, & r < 1 - \dfrac{1}{2b}, \\ 0, & 1 - \dfrac{1}{2b} \le r \le 1 + \dfrac{1}{b}, \\ 2\varepsilon, & 1 + \dfrac{1}{b} < r. \end{cases} \tag{33}$$

The motivation of this choice is that $-1/2b$ and $1/b$ are characteristic length scales for the exponential increase of $V(r)$ in the vicinity of the minimum at $r = 1$ and, secondly, $V_B(r)$ provides for exact further calculations. More exactly, we shall see, that the use of $V_B(r)$ leads to satisfactory analytical results, if $\gamma_0 \ll b$ holds (in c.u.), i.e., if the conservative forces dominate the collision process.

Considering $V_B(r)$ and, like before, initial conditions $v_r(0) = -2\sqrt{\mu}$ and $r(0) = 20\sigma$ the quasi-particle arrives at $r_1 = 1 + 1/b \le r$ with exactly the same speed, $v_r^+(r_1) = -2\sqrt{\mu}$, corresponding to the kinetic energy value

$$T_r^+(r_1) = 2\mu. \tag{34}$$

While passing through r_1 the quasi-particle gains additional kinetic energy from the step of the potential energy leading to

$$T_r^-(r_1) = 2\mu + 2 \Rightarrow v_r^-(r_1) = -2\sqrt{\mu + 1}. \tag{35}$$

Consequently, from this point on the quasi-particle is subject to the nonlinear friction force. Since its absolute velocity is bigger than $2\sqrt{\mu}$, it is effectively slowed down by the friction. The dynamical equations for the motion of the quasi-particle in $V_B(r)$ between r_1 and $r_2 = 1 - 1/2b$ are given by

$$\dot{r} = v_r, \tag{36a}$$

$$\dot{v}_r = \gamma_0 \frac{4\mu - v_r^2}{4\kappa + v_r^2} v_r. \tag{36b}$$

The quasi-particle moves on until it reaches r_2, there it is reflected and returns to r_1. The stationary bound state of the original collision process corresponds to the situation, where the energy loss of the quasi-particle due to the friction is large enough to prevent it from overcoming the step of the potential $V_B(r)$ at r_1. In other words, when it has returned to r_1 its kinetic energy $T_r^{\mathrm{ret}}(r_1)$ has to be smaller than the critical value $T^c := 2\varepsilon$ or, respectively, in c.u.

$$T_r^{\mathrm{ret}}(r_1) < T^c = 2 \Rightarrow v_r^{\mathrm{ret}}(r_1) < v_r^c = 2. \tag{37}$$

Otherwise the quasi-particle escapes over the potential barrier and we observe a quasi-elastic collision. The critical energy-loss

$$\Delta E^c := T_r^-(r_1) - T^c = 2\mu \tag{38}$$

is connected to a critical parameter value $\gamma_0^c = \gamma_0^c(b, \mu, \kappa)$ and this is the quantity we intend to calculate now. We note, that (38) simply means that the quasi-particle has to loose its full amount of initial kinetic energy in order to achieve a bound state. The reflection at r_2 is assumed to be elastic and thus it can be taken into account by simply extending the range of validity of (36) to the interval $(1 + 1/b, 1 - 2/b)$ as long as we also change the sign of the boundary value

$$v_r^c = 2 \to \tilde{v}_r^c = -2. \tag{39}$$

Dividing the first equation in (36) by the second, separation of variables and consideration of all relevant boundary conditions gives

$$\int_{1+1/b}^{1-2/b} \mathrm{d}r = \frac{1}{\gamma_0^{\mathrm{c}}} \int_{-2\sqrt{\mu+1}}^{\tilde{v}_r^{\mathrm{c}}} \mathrm{d}v_r \frac{4\kappa + v_r^2}{4\mu - v_r^2}, \tag{40}$$

and thus

$$\gamma_0^{\mathrm{c}} = \frac{2b}{3} \left\{ \sqrt{\mu+1} - 1 + \frac{\kappa+\mu}{\sqrt{\mu}} \left[\operatorname{arccoth}(\sqrt{\mu}) - \operatorname{arctanh}\left(\sqrt{\frac{1+\mu}{\mu}} \right) \right] \right\}. \tag{41}$$

This function has a pole at $\mu = 1$ reflecting the fact that for the initial conditions applied here bound states can only exist as long as the kinetic energy provided by the negative friction is smaller than the binding energy 2ε. However, if we compare the numerically calculated curve 1 in Fig. 7 with the graph of (41) given by curve 4, then the analytic expression (41) represents an appropriate approximation only for the lower part of the numerically simulated γ_0^{c}-curve. Hence, the remainder of this section is dedicated to the upper part. This branch corresponds to the parameter constellation $\gamma_0 \gg b$ (in c.u.), where the dissipative forces dominate the dynamics. Obviously, in this parameter region the approximation of the effective potential $V(r) = 2U(r)$ by means of the box-potential (33) is not sufficient anymore in order to explain the results of the computer experiments correctly. Before we discuss a more successful alternative, it is convenient to give some more general statements concerning this parameter regime. In principle, we can still use the quasi-particle model introduced above. From the qualitative point of view, the motion of quasi-particle is similar as before. Incoming from the right it passes through the minimum of the effective potential $V(r)$ at $r = 1$ (in c.u.) and is reflected at some point $r_2 < 1$. Finally, it returns at time t_1 to the minimum. Now we make our first essential assumption. Remembering $\gamma_0 \gg b$, we can assume that at this time the quasi-particle's velocity is given by $v_r(t_1) \approx 2\sqrt{\mu}$ due to the dominating (effective) friction force

$$f_{\mathrm{dis}}^{\mathrm{eff}}(v_r) := \gamma_0 \frac{4\mu - v_r^2}{4\kappa + v_r^2} v_r. \tag{42}$$

This also means, that we can neglect all the previous dynamics at $t < t_1$. Consequently, we begin our quantitative analysis at $t = t_1$ and $r = 1$. In order to obtain analytical results, we now approximate the original effective potential $V(r)$ for $r \geq 1$ by

$$V_{\mathrm{L}}(r) = \begin{cases} \dfrac{2b}{3}(r-1), & 1 \leq r \leq 1 + \dfrac{3}{b} =: r_2, \\ 2, & 1 + \dfrac{3}{b} < r. \end{cases} \tag{43}$$

The piecewise linear potential $V_{\mathrm{L}}(r)$ is chosen such that

$$V_{\mathrm{L}}(1) = V(1) = 0, \qquad V_{\mathrm{L}}(\infty) = V(\infty) = 2, \qquad \int_1^\infty \mathrm{d}r |V_{\mathrm{L}}(r) - V(r)| = 0.$$

Furthermore, we approximate the effective friction force (42) by using a linear friction coefficient

$$f_{\mathrm{dis}}^{\mathrm{eff}}(v_r) \approx \gamma_0 \frac{\mu}{\kappa}(2\sqrt{\mu} - v_r) v_r, \tag{44}$$

yielding the modified dynamical equations

$$\dot{r} = v_r, \tag{45a}$$

$$\dot{v}_r = -\frac{2b}{3} + \gamma_0 \frac{\mu}{\kappa}(2\sqrt{\mu} - v_r)v_r, \tag{45b}$$

for the motion of the quasi-particle between $r(t_1) = 1$ and $r_2 = 1 + 3/b$. Again a separated state [1, 1] is observed only if the quasi-particle can escape from the potential well to $r = \infty$. Considering $V_L(r)$, this only happens if $v_r(r_2) > 0$. Hence, by analogy to (40) the connected critical parameter value γ_0^c can be determined from

$$\int_1^{r_2} \mathrm{d}r = \int_{2\sqrt{\mu}}^{0} \mathrm{d}v_r \frac{v_r}{\gamma_0(\mu/\kappa)(2\sqrt{\mu} - v_r)v_r - 2b/3}. \tag{46}$$

Evaluation of the integrals gives the following transcendental equation for γ_0^c:

$$\frac{3}{b} = 2\kappa\sqrt{\frac{3}{\gamma_0^c}} \frac{\arctan(\sqrt{3\gamma_0^c}\mu/\sqrt{2b\kappa - 3\gamma_0^c\mu^2})}{\sqrt{2b\kappa - 3\gamma_0^c\mu^2}}, \tag{47}$$

which can be solved numerically (see curve 2 in Fig. 7). Moreover, one can still get, e.g., from the denominator in (47), the following upper boundary

$$\gamma_0^c \leq \frac{2b\kappa}{3\mu^2}. \tag{48}$$

The r.h.s. of this inequality is illustrated as curve 3 in Fig. 7. Together with curve 4 corresponding to the graph of the complementary estimate (41) we thus have achieved a satisfactory analytical confirmation of the numerical results.

Finally, we can summarize the results of this section. For the initial conditions applied in this work, the dissipative collision of two active particles can only lead to two different stationary states. The first one corresponds to a bound state, $[N] = [2]$, with vanishing c.o.m. velocity. In this state the two particles perform optical oscillations. The second stationary state, $\phi = [1, 1]$, is characterized by two particles moving away from each other after the collision. Hence, the process leading to this state can be interpreted as a quasi-elastic collision. The parameter regions leading to the different final states could be analytically estimated.

4. Numerical results for $N > 2$

In principle, it is not necessary to investigate the collision of an initial state $\phi'_{\mathrm{in}} = [N_2, N_1]$, if the the opposite case of a $\phi_{\mathrm{in}} = [N_1, N_2]$ collision has been investigated before. This is due to the fact that the dynamics of these two cases is connected by the transformation

$$v'_i(t) = -v_{N-i+1}(t), \qquad x'_i = x_N(0) - x_{N+1-i}(t). \tag{49}$$

In terms of fragmentation channels this simply means that if ϕ_{in} leads to a final state $\phi = [n_1, \ldots, n_j]$, then ϕ'_{in} leads to $\phi' = [n'_1, \ldots, n'_j] = [n_j, \ldots, n_1]$.

In Figs. 8–10 we plotted the results of the computer simulations for systems with $N = 3$, 4 and 8 particles. The case $N = 4$ is the first case, where symmetric initial conditions $[N_1, N_2]$ with $N_1 = N_2$ as well as asymmetric initial conditions $[N_1, N_2]$ with $N_1 \neq N_2$ can be investigated. In principle, we observe only two different types of stationary states. Either the two colliding chains $[N_1, N_2]$ merge with each other and the result is one big cluster (or bound state) $[N]$ or, otherwise, they split again into a cluster configuration $[N_2, N_1]$. The latter case can be interpreted as quasi-elastic collisions. Furthermore, we can learn from the case $N = 4$ that the μ–γ_0-parameter region, where the fusions occur, depends on the initial distribution of the particles in the clusters. According to our numerical results, this region becomes considerably smaller for the symmetric initial state (see Fig. 9). The same

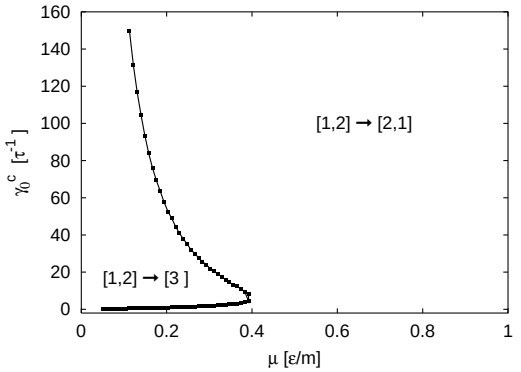

Fig. 8. Fragmentation channels for $N = 3$ with asymmetric initial state $[N_1, N_2] = [1, 2]$. Further parameter values are $b = 5$, $\kappa = 1$ (in c.u.). The results are very similar to those obtained for $N = 2$ and $N = 4$.

tendency is observable for $N = 8$ particles (Fig. 10). Another new effect appearing for particle numbers $N > 2$ is shown in Fig. 11. In contrast to the process

$$[1, 1] \to [2] \tag{50}$$

discussed in the previous section, we can now distinguish between stationary bound states, $[N]_{v_s}$, with vanishing and non-vanishing c.o.m. velocity

$$v_s := \frac{1}{N}\sum_{i=1}^{N} v_i \quad \text{(in c.u.)}. \tag{51}$$

Depending on the parameter values b, κ, γ_0, μ and initial configurations, $[N_1, N_2]$, there exist three possible stationary values

$$v_s(\infty) := \lim_{t\to\infty} v_s(t) \in \{0, \pm\sqrt{\mu}\}. \tag{52}$$

If the stationary state $[N]_{v_s(\infty)=0}$ is approached, then the particles perform stationary relative oscillations around the equilibrium distance $r = \sigma = 1$ (in c.u.) as represented in Fig. 11(a) and already discussed for $N = 2$ in the

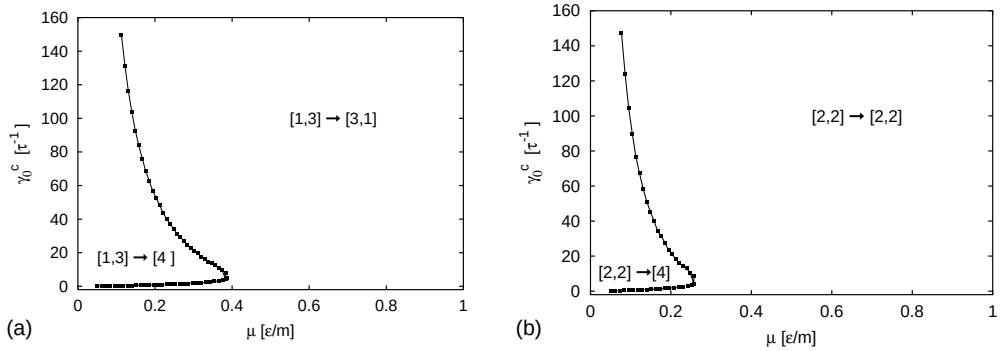

Fig. 9. Fragmentation channels for $N = 4$ with (a) asymmetric initial state [1, 3] and (b) symmetric initial state [2, 2]. Further parameter values are $b = 5$, $\kappa = 1$ (in c.u.). For the asymmetric initial condition in (a) the parameter region leading to a fusion is significantly larger compared with the symmetric initial state.

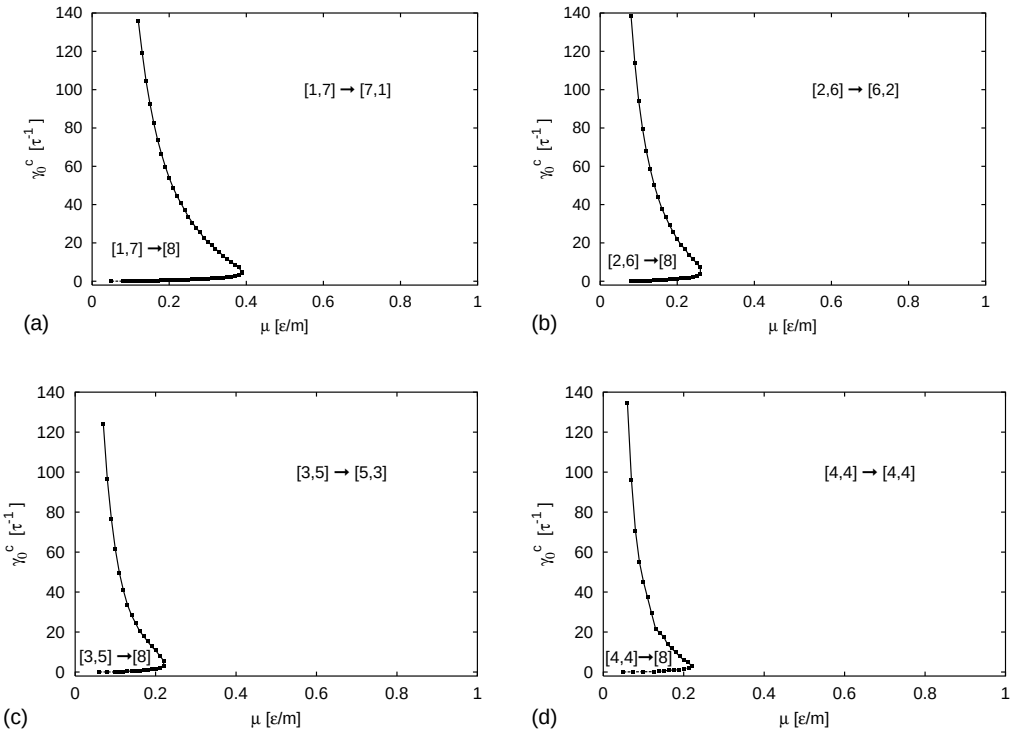

Fig. 10. Fragmentation channels for $N = 8$ and different initial states $[N_1, N_2]$. As already observed for $N = 4$, the parameter region leading to a fusion decreases with increasing symmetry of the initial state. Further parameter values are $b = 5$, $\kappa = 1$ (in c.u.).

previous section (see also Fig. 6). On the other hand, if the fragmentation channel $[N]_{\pm\sqrt{\mu}}$ represents the stationary state, then the relative oscillations are damped out and all particles move into the same direction with constant distances $r = \sigma$ between each other. It is not difficult to show [13], that these stationary configurations correspond to stable fixed points of the dynamical system (1). Due to the special initial conditions used throughout this work, the stationary states $[N]_{\pm\sqrt{\mu}}$, as shown in Fig. 11(b), can only be observed in case of asymmetric initial states, since

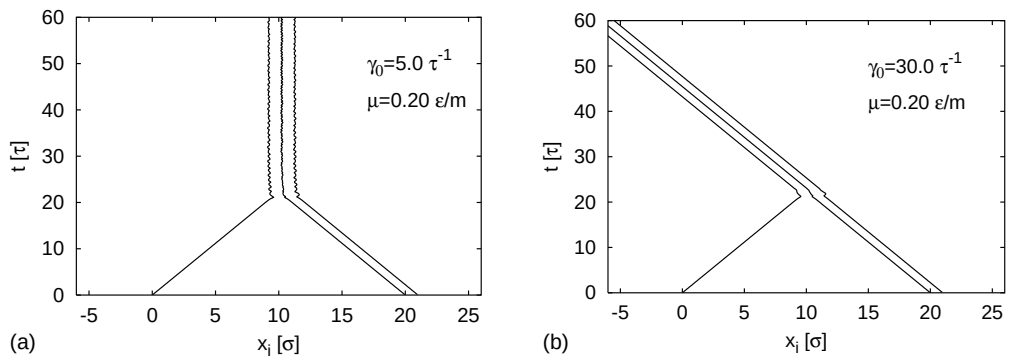

Fig. 11. Two different realizations of the fragmentation channel $[N] = [3]$ characterized by different stationary c.o.m. velocities $v_s(\infty)$. (a) A process leading to a stationary configuration with $v_s(\infty) = 0$. (b) A fusion with stationary c.o.m. velocity $v_s(\infty) = -\sqrt{\mu}$. Further parameter values are $b = 5$, $\kappa = 1$ (in c.u.).

otherwise the c.o.m. velocity is conserved. We emphasize, that this conservation of the c.o.m. velocity is a special property of our model, which only holds in presence of highly symmetric initial conditions.

For the sake of completeness we note, that we extended our simulations on parameter values $\mu \gg 1$, but this did not lead to any new effects.

5. Conclusions and outlook

According to our numerical results, we can observe two qualitatively different types of dissipative collision processes for arbitrary particle particle numbers N in our model. More exactly, these are fusions described by

$$[N_1, N_2] \to [N], \tag{53}$$

and quasi-elastic collisions

$$[N_1, N_2] \to [N_2, N_1]. \tag{54}$$

Identical initial conditions (i.e., same initial energy per particle, distances and configuration $[N_1, N_2]$) can lead to both types of processes, if the parameters (e.g. the viscous friction coefficient γ_0) of the system are varied accordingly.

The hyperplane, which separates the two processes in the parameter space, can be analytically estimated for the simplest case $N = 2$. For particle numbers $N > 2$ its shape seems to be qualitatively similar, but quantitatively it also depends on the initial configuration $[N_1, N_2]$. Considering the numerical simulations, it seems likely that the parameter region leading to fusion decreases for more symmetric initial states.

In previous studies of dissipative collision models [8,9], the effects of a linear friction force of type

$$f_{\text{dis}} = \begin{cases} \gamma_0(v_{i+1} - v_i), & \text{if } |x_{i+1} - x_i| < d_{\text{crit}}, \\ 0, & \text{otherwise}, \end{cases} \tag{55}$$

acting on the relative velocity of n.n. were investigated. In the mentioned articles, the authors used a similar class of initial conditions but found a significantly higher number of different fragmentation channels than we do here. In order to explain this difference, it is useful to remember the close relationship between the stable states of the dissipative potential U_{dis} introduced in Section 2.2 and the stationary states of the collision experiments. While in our model there exist only a limited number of stable states of U_{dis}, corresponding to velocity values $v(0) = \pm\sqrt{\mu}$, the dissipative potential $\tilde{U}_{\text{dis}}$ connected with (55) shall possess a continuous set of minima in the velocity space, merely determined by the condition $v_i = v_{i+1}$, if the distance between n.n. is smaller than a critical value d_{crit}.

Thus, as a general result, we may conclude, that (i) the presence of dissipative forces may increase the variety of possible fragmentation pattern compared with the case of purely conservative interactions and (ii) the number of observable fragmentation channels essentially depends on the structure of the dissipative terms appearing in the equations of motions.

Since the methods applied in the above sections are independent from the rather simple and academic model discussed in this paper, we will extend our studies on more realistic models of dissipative collision processes in the near future. Due to the fact that the results are obviously very sensitive with regard to the form of the dissipative terms, one of the primary tasks will be the finding of a realistic dissipation model. Attempts to solve this problem could, for example, also include stochastic pumping effects in the equations of motions. More exactly, one could think of random forces modeling thermal fluctuations.

Acknowledgements

The authors are grateful to the German Ministry of Science and Education (BMBF), the Deutsche Forschungsgemeinschaft (DFG/Sfb555) and the Studienstiftung des deutschen Volkes (J.D.) for financial support.

References

[1] T. Mayer-Kuckuk, Kernphysik, Teubner, Stuttgart, 1984.
[2] D.H.E. Gross, Rep. Prog. Phys. 53 (1990) 605.
[3] D.H.E. Gross, Rep. Prog. Phys. 279 (1997) 119.
[4] R. Schmidt, H.O. Lutz, R. Dreizler (Eds.), Nuclear Physics Concepts in the Study of Atomic Clusters, Lecture Notes in Physics, vol. 404, Springer, Berlin, 1994.
[5] L.D. Landau, E.M. Lifshits, Theoretical Physics, 3rd ed., vol. 1/3, Butterworths–Heinemann, London, 1981/1982.
[6] V.V. Volkov, Nuclear Reactions in Inelastic Collisions, Energoizdat, Moscow, 1982 (in Russian).
[7] R. Feistel, W. Ebeling, Evolution of Complex Systems, Kluwer Academic Publishers, Dordrecht, 1989.
[8] J.W.P. Schmelzer, G. Röpke, R. Mahnke (Eds.), Self-organization in multifragmentation in atomic and nuclear collision processes, in: Aggregation Phenomena in Complex Systems, Wiley/VCH, Weinheim, 1999.
[9] W. Kleinig, J.W.P. Schmelzer, G. Röpke, Fragmentation in dissipative collisions: a computer model study, Physica D 164 (2002) 110.
[10] F. Schweitzer, W. Ebeling, B. Tilch, Complex motion of Brownian particles with energy depots, Phys. Rev. Lett. 80 (23) (1998) 5044.
[11] J.W. Rayleigh, The Theory of Sound, 2nd ed., vol. 1, Dover, New York, 1945.
[12] J. Dunkel, W. Ebeling, U. Erdmann, Thermodynamics and transport in active Morse chains, Eur. Phys. J. B 24 (2001) 511.
[13] J. Dunkel, W. Ebeling, U. Erdmann, V.A. Makarov, Coherent motions and clusters in a dissipative Morse ring chain, Int. J. Bifurc. Chaos 12 (2002) 2359.
[14] P. Morse, Diatomic molecules according to the wave mechanics. II. Vibrational levels, Phys. Rev. 34 (1929) 57.
[15] M. Toda, Nonlinear Waves and Solitons, Kluwer Academic Publishers, Dordrecht, 1983.
[16] W. Ebeling, U. Erdmann, J. Dunkel, M. Jenssen, Nonlinear dynamics and fluctuations of dissipative Toda chains, J. Stat. Phys. 101 (2000) 443, and references therein.
[17] W. Ebeling, Nonlinear excitations and statistical theory of systems of Brownian particles with energy supply, in: Proceedings of the International Conference on Chaos in Dynamical Systems, Mizdroy, Poland, May 2001, p. 17.